HHS Public Access

Author manuscript

Apoptosis. Author manuscript; available in PMC 2016 November 01.

Published in final edited form as:

Apoptosis. 2011 August ; 16(8): 769–782. doi:10.1007/s10495-011-0609-x.

Hydroxyl radical mediates cisplatin-induced apoptosis in human hair follicle dermal papilla cells and keratinocytes through Bcl-2-dependent mechanism

Sudjit Luanpitpong,
Faculty of Pharmaceutical Sciences, Chulalongkorn University, Bangkok 10330, Thailand

Department of Pharmaceutical Sciences, West Virginia University, P.O. Box 9530, Morgantown, WV 26506, USA

Ubonthip Nimmannit,
National Nanotechnology Center, National Science and Technology Development Agency, Pathumthani 12120, Thailand

Pithi Chanvorachote,
Faculty of Pharmaceutical Sciences, Chulalongkorn University, Bangkok 10330, Thailand

Stephen S. Leonard,
Pathology and Physiology Research Branch, National Institute for Occupational Safety and Health, Morgantown, WV 26506, USA

Varisa Pongrakhananon,
Faculty of Pharmaceutical Sciences, Chulalongkorn University, Bangkok 10330, Thailand

Department of Pharmaceutical Sciences, West Virginia University, P.O. Box 9530, Morgantown, WV 26506, USA

Liying Wang, and
Pathology and Physiology Research Branch, National Institute for Occupational Safety and Health, Morgantown, WV 26506, USA

Yon Rojanasakul
Department of Pharmaceutical Sciences, West Virginia University, P.O. Box 9530, Morgantown, WV 26506, USA

Ubonthip Nimmannit: Ubonthip.N@chula.ac.th; Yon Rojanasakul: yrojan@hsc.wvu.edu

Abstract

Induction of massive apoptosis of hair follicle cells by chemotherapy has been implicated in the pathogenesis of chemotherapy-induced alopecia (CIA), but the underlying mechanisms of regulation are not well understood. The present study investigated the apoptotic effect of cisplatin in human hair follicle dermal papilla cells and HaCaT keratinocytes, and determined the identity and role of specific reactive oxygen species (ROS) involved in the process. Treatment of the cells with cisplatin induced ROS generation and a parallel increase in caspase activation and apoptotic

Correspondence to: Ubonthip Nimmannit, Ubonthip.N@chula.ac.th; Yon Rojanasakul, yrojan@hsc.wvu.edu.

cell death. Inhibition of ROS generation by antioxidants inhibited the apoptotic effect of cisplatin, indicating the role of ROS in the process. Studies using specific ROS scavengers further showed that hydroxyl radical, but not hydrogen peroxide or superoxide anion, is the primary oxidative species responsible for the apoptotic effect of cisplatin. Electron spin resonance studies confirmed the formation of hydroxyl radicals induced by cisplatin. The mechanism by which hydroxyl radical mediates the apoptotic effect of cisplatin was shown to involve down-regulation of the anti-apoptotic protein Bcl-2 through ubiquitin-proteasomal degradation. Bcl-2 was also shown to have a negative regulatory role on hydroxyl radical. Together, our results indicate an essential role of hydroxyl radical in cisplatin-induced cell death of hair follicle cells through Bcl-2 regulation. Since CIA is a major side effect of cisplatin and many other chemotherapeutic agents with no known effective treatments, the knowledge gained from this study could be useful in the design of preventive treatment strategies for CIA through localized therapy without compromising the chemotherapy efficacy.

Keywords

Alopecia; Apoptosis; Cisplatin; Hair follicle; Reactive oxygen species; Toxicity

Introduction

Chemotherapy-induced alopecia (CIA), an induction of massive hair loss by chemotherapy, remains an unresolved problem in clinical oncology [1]. More than 80% of cancer chemotherapy patients consider CIA as the most distressing side effect, leading to poor therapeutic outcome [2, 3]. Incidence of the disease varies depending on the type of drugs, their dosage, and route of administration. Progressive understanding in CIA has been achieved using rodent models. Substantial evidence suggests that various chemotherapeutic agents induce massive apoptosis in several hair follicle compartments, including dermal papilla and matrix keratinocytes, and cause alopecia [4–6]. Despite such understanding, the mechanisms underlying the disease process remains obscure and effective preventive treatment has yet to be developed.

Cisplatin (*cis*-diamminedichloroplatinum) is a commonly used chemotherapeutic agent for a variety of human cancers with a high potential to induce alopecia [4, 7]. Induction of ROS generation by cisplatin is considered to be one of the mechanisms of cancer cell death [8, 9]. Accumulating evidence also indicates the involvement of ROS in the toxic side effects of cisplatin including ototoxicity and nephrotoxicity [10–12]. Certain antioxidants such as lycopene, lipoic acid, and dimethyl thiourea have been shown to alleviate these toxic effects of cisplatin [13–15]. To date, the mechanisms by which cisplatin causes hair follicle toxicity and its regulation by ROS have not been demonstrated. Cisplatin has been shown to induce apoptosis mainly through the mitochondrial (intrinsic) death pathway [9, 16]. The intrinsic death pathway involves the release of cytochrome *c* from mitochondria, which then binds to caspase-activating proteins such as Apaf-1 and initiates the caspase cascade leading to apoptosis [17, 18]. The induction of apoptosis through the intrinsic death pathway is regulated primarily by Bcl-2 family proteins, notably the pro-apoptotic Bax and anti-apoptotic Bcl-2 proteins. It is generally accepted that Bcl-2 protects cells from apoptosis and

that the activity of Bcl-2 is determined by its interaction with Bax. The release of cytochrome *c* from mitochondria and subsequent cell death is prevented when Bax forms heterodimers with Bcl-2 [19, 20]. Thus, in contrast to Bcl-2, the elevated level of Bax promotes apoptotic cell death. Interestingly, Bcl-2 and Bax were previously shown to regulate hair follicle apoptosis during apoptosis-driven regression phase of hair cycle (catagen) [21, 22]. The coincidental decline of Bcl-2 level with an increase of Bax level was detected in hair matrix keratinocytes undergoing apoptosis. These findings have led to the hypothesis that ROS may function as a key mediator of cisplatin-induced apoptosis in hair follicle cells by regulating Bcl-2 and Bax levels.

The observation that Bcl-2 is often expressed at a high level in apoptosis-resistant cells [23, 24] underlines the significance of Bcl-2 in the apoptotic process. Bcl-2 expression is tightly regulated by different mechanisms, including transcription, dimerization, and degradation. Degradation of Bcl-2 is mediated primarily through the ubiquitin-proteasomal pathway [25, 26], which was previously reported to play an important role in apoptosis induced by various cytotoxic agents [9, 27, 28]. In the present study, we investigated the susceptibility of human hair follicle cells to apoptotic cell death induced by cisplatin using human hair follicle dermal papilla cells (HFDPC) and HaCaT keratinocytes. The HaCaT cells were used experimentally as they expressed an epidermal phenotype similarly to the outer root sheath cells of hair follicles [29]. We also investigated the mechanisms of apoptotic cell death and the role of ROS and Bcl-2 family proteins in the process.

Materials and methods

Cell culture

Human HFDPC were obtained from PromoCell (Heidelberg, Germany). The cells were cultured in DP cell growth medium (PromoCell) containing 100 units/ml of penicillin and 100 μg/ml of streptomycin (Gibco, Gaithersburg, MA, USA) in a 5% CO_2 environment at 37°C. Human keratinocyte HaCaT cells were obtained from Cell Lines Service (Heidelberg, Germany) and maintained in Dulbecco's modified Eagle's medium (DMEM) (Gibco, Gaithersburg, MA) supplemented with 2 mM L-glutamine and 10% fetal bovine serum in a 5% CO_2 at 37°C.

Reagents

Cis-diamminedichloroplatinum II (cisplatin, CDDP), 3-(4, 5-dimethylthiazol-2-yl)-2,5-diphenyltetrazolium bromide (MTT), *N*-acetyl cysteine (NAC), reduced glutathione (GSH), sodium formate, uric acid, lactacystin, and antibody for ubiquitin were obtained from Sigma Chemical, Inc. (St. Louis, MO). Hoechst 33342 and dihydrodichlorofluorescein diacetate (H_2DCF-DA) were obtained from Molecular Probes, Inc. (Eugene, OR). Mn(III)tetrakis(4-benzoic acid) porphyrin chloride (MnTBAP) and concanamycin A (CMA) were obtained from EMD Biosciences, Inc. (La Jolla, CA). Caspase inhibitor benzyloxycarbonyl-Val-Ala-Asp-(OMe) fluoromethyl ketone (zVA D-fmk) was obtained from Alexis Biochemicals (San Diego, CA). Hydroxyphenyl fluorescein (HPF) was obtained from Cell Technology (Mountain View, CA). Antibody for Bcl-2 and protein G-conjugated agarose were obtained from Santa Cruz Biotechnology (Santa Cruz, CA). Antibodies for Bax, procaspase-3, β-

actin, and peroxidase-conjugated secondary antibodies were obtained from Cell Signaling Technology (Boston, MA).

Plasmids and transfection

Bcl-2 plasmid was generously provided by Dr. C. Stehlik (Northwestern University, School of Medicine, Chicago, IL). Authenticity of the plasmid construct was verified by DNA sequencing. Cells were transfected with Bcl-2 or pcDNA3 control plasmid by nucleofection using Amexa Biosystems Nucleofector (Cologne, Germany), according to the manufacturer's instruction. Briefly, cells were suspended in 100 μl of nucleofection solution with 2 μg of plasmid and nucleofected using the device program U020. The cells were then resuspended in 500 μl of complete medium and seeded in 6-mm cell culture dish. Cells were allowed to recover for 72 h before each experiment. The efficiency of transfection was determined by using a GFP reporter plasmid and was found to be approximately 85%.

ROS detection

Reactive oxygen species generation was determined by flow cytometry using dichlorodihydrofluorescein diacetate (H_2DCF-DA) as a fluorescent probe. Briefly, cells were incubated with the probe (10 μM) for 30 min at 37°C, after which they were washed, resuspended in phosphate-buffered saline (PBS) and immediately analyzed for fluorescence intensity by flow cytometry using a 485-nm excitation beam and a 538-nm band-pass filter (FACSort, Becton–Dickinson, Rutherford, NJ). The mean fluorescence intensity was quantified by CellQuest software (Becton–Dickinson) analysis of the recorded histograms.

Generation of highly reactive oxygen species (hROS) was determined according to the method previously described [30] using HPF as a probe. Briefly, cells were incubated with the probe (10 μM) for 1 h at 37°C, after which they were washed, resuspended in Hank's buffered salt solution (HBSS) and analyzed for fluorescence intensity using a fluorescence plate reader at a 485-nm excitation and a 520-nm emission (FLUOstar OPTIMA, BMG Labtech, Durham, NC).

Electron spin resonance (ESR) measurements were performed to identify specific ROS. Cells were incubated with 5,5-dimethyl-1-pyrroline-*N*-oxide (DMPO, 10 mM) for 10 min at 37°C in the presence or absence of ROS modulators. ESR signals were measured using a Bruker EMX spectrometer (Bruker Instruments, Billerica, MA) and a flat cell assembly. Hyperfine couplings were measured (to 0.1 G) directly from magnetic field separation using potassium tetraperoxochromate and 1,1-diphenyl-2-picrylhydrazyl as reference standards. An Acquisit program (Bruker Instruments) was used for data acquisition and analysis.

Cytotoxicity and apoptosis assays

Cytotoxicity was determined by MTT colorimetric assay. After specific treatments, cells in 96-well plate were incubated with 500 μg/ml of MTT for 4 h at 37°C. The intensity of the formazan product was measured at 550 nm using a microplate reader. Relative cell viability was calculated by dividing the absorbance of treated cells by that of the non-treated cells in each experiment. Apoptosis was determined by Hoechst 33342 DNA fragmentation assay. Briefly, cells were incubated with 10 μg/ml of Hoechst 33342 for 30 min and analyzed for

apoptosis by scoring the percentage of cells having intensely condensed chromatin and/or fragmented nuclei by fluorescence microscopy (Leica Microsystems, Bannockburn, IL). Approximately 1,000 nuclei from ten random fields were analyzed for each sample. The apoptotic index was calculated as the percentage of cells with apoptotic nuclei over total number of cells.

Western blot analysis

After specific treatments, cells were incubated with lysis buffer containing 20 mM Tris–HCl (pH 7.5), 1% Triton X-100, 150 mM NaCl, 10% glycerol, 1 mM Na_3VO_4, 50 mM NaF, 100 mM phenylmethylsulfonyl fluoride, and a commercial protease inhibitor mixture (Roche Molecular Biochemicals) at 4°C for 20 min. Cell lysates were collected and determined for protein content using the Bradford method (Bio-Rad Laboratories, Hercules, CA). Proteins (40 μg) were resolved under denaturing conditions by 10% sodium dodecyl sulfate-polyacrylamide gel electrophoresis (SDS-PAGE) and transferred onto nitrocellulose membranes (Bio-Rad). The transferred membranes were blocked for 1 h in 5% nonfat dry milk in TBST (25 mM Tris–HCl, pH 7.4, 125 mM NaCl, 0.05% Tween 20) and incubated with appropriate primary antibodies at 4°C overnight. Membranes were washed twice with TBST for 10 min and incubated with horseradish peroxidase-coupled isotype-specific secondary antibodies for 1 h at room temperature. The immune complexes were detected by enhanced chemiluminescence detection system (Amersham Biosciences, Piscataway, NJ) and quantified using analyst/PC densitometry software (Bio-Rad Laboratories, Hercules, CA).

Caspase-3 activity assay

Caspase activity was measured by using APO LOGIX carboxyfluorescein caspase detection kit (Cell Technologies, Minneapolis, MN), according to the manufacturer's instructions. After specific treatments, cells were incubated with 10 μl of 30× FAM-DEVD-fmk for 2 h in dark. Cells were washed with 1× Working Dilution Wash Buffer which was supplied with the kit. The fluorescence signals were measured using a fluorescence microplate reader at the excitation and emission wavelengths of 488 and 520 nm, respectively. Caspase activity was expressed as the ratio of fluorescence signal from the treated and control samples.

Immunoprecipitation

After specific treatments, cells were washed with PBS and lysed in lysis buffer at 4°C for 20 min. The lysates were collected and determined for protein content using the Bradford method (Bio-Rad Laboratories). Cell lysates (60 μg protein) were incubated with anti-Bcl-2 antibody at 4°C for 14 h, followed by incubation with protein G-conjugated agarose for 4 h at 4°C. The immune complexes were washed 6 times with cold lysis buffer and resuspended in 2× Laemmli sample buffer. The immune complexes were separated by 10% SDS-PAGE and analyzed by western blotting as described.

Statistical analysis

The data represent means ± SD from three or more independent experiments. Statistical analysis was performed by Student's *t* test at a significance level of $P < 0.05$.

Results

Cisplatin induces apoptosis of HFDPC and keratinocytes

Cisplatin has been shown to induce hair loss under clinical applications [4, 7]. To determine the mechanisms of cisplatin-induced hair loss, we first evaluated the cytotoxic effect of cisplatin on human HFDPC and HaCaT keratinocytes. The cells were treated with various concentrations of cisplatin and their viability was determined by MTT assay. Figure 1a and b shows that cisplatin dose-dependently decreased the viability of both HFDPC and HaCaT cells. This effect of cisplatin was inhibited by pan-caspase inhibitor, zVAD-fmk, in both cell types, suggesting caspase-dependent apoptosis as the mechanism of cisplatin-induced cytotoxicity. Apoptosis assays show that cisplatin was able to induce apoptosis of both HFDPC and HaCaT cells and that this effect can be inhibited by co-treatment of the cells with antioxidants such as reduced glutathione (GSH) and NAC (Fig. 1c, d). These results suggest the role of ROS in the apoptosis induction by cisplatin, which is confirmed in subsequent studies using specific ROS scavengers. Figure 1e and f shows representative micrographs of the cells treated with cisplatin in the presence or absence of NAC.

Cisplatin induces ROS generation in HFDPC and HaCaT cells

To provide evidence for cisplatin-induced ROS generation, HFDPC and HaCaT cells were treated with cisplatin in the presence or absence of antioxidant NAC, and cellular ROS levels were determined by flow cytometry and fluorescence microscopy using H_2DCF-DA as a fluorescent probe. Time course measurements of ROS generation were first analyzed and found the maximum response time of 2 h. Figure 2a and b shows that cisplatin was able to induce ROS generation, as indicated by the increase in cellular DCF fluorescence intensity which was inhibited by the addition of antioxidant NAC. Figure 2c and d shows representative results of the flow cytometry and microscopy experiments which support the generation of ROS in cisplatin-treated HFDPC and HaCaT cells.

Role of specific ROS in cisplatin-induced apoptosis

To determine the role of specific ROS in cisplatin-induced apoptosis, HFDPC and HaCaT cells were treated with cisplatin in the presence or absence of various specific ROS scavengers, including catalase (CAT) (hydrogen peroxide scavenger), MnTBAP (MnSOD mimetic and superoxide anion scavenger) and sodium formate (hydroxyl radical scavenger), and apoptosis was determined by Hoechst 33342 assay. Figure 3a and b shows that CAT and MnTBAP had no significant effect on apoptosis induced by cisplatin, whereas sodium formate strongly inhibited the apoptosis. Analysis of ROS generation by flow cytometry also indicated that sodium formate inhibited the generation of ROS induced by cisplatin, whereas CAT and MnTBAP had no significant inhibitory effect (Fig. 3c, d). These results suggest that hydroxyl radical is a major ROS produced by the cells in response to cisplatin treatment and that this oxidative species plays a key role in apoptosis induced by cisplatin. The important role of hydroxyl radical in the apoptotic process was substantiated by the observation that another known inhibitor of hydroxyl radical, deferoxamine, also protected the cells from cisplatin-induced apoptosis (data not shown).

To confirm the formation of hydroxyl radicals in response to cisplatin treatment, two additional experiments were performed. First, HPF was used as a probe to detect highly reactive oxygen species in the presence or absence of hydroxyl radical scavenger sodium formate. Upon treatment of the cells with cisplatin, cellular HPF fluorescence intensity was enhanced in a dose-dependent manner, the effect that was completely inhibited by sodium formate (Fig. 3e, f). Secondly, ESR measurements using spin trapping agent DMPO were performed. In response to cisplatin treatment, an ESR signal consisting of a 1:2:2:1 quartet which is a characteristic of DMPO-$OH^{\bullet}$ adduct was observed (Fig. 4a). Addition of sodium formate, but not MnTBAP or CAT, to the treated cells inhibited the ESR signal, indicating the scavenging of hydroxyl radical under the test condition. Since hydrogen peroxide is a major source of hydroxyl radical, the lack of inhibitory effect of CAT on cisplatin-induced hydroxyl radical formation is somewhat surprising and suggests other unknown sources of hydroxyl radical. Recently, it has been reported that hydroxyl radical could be formed from the decomposition of peroxynitrite [31, 32]. To test this possibility, we utilized a known specific scavenger of peroxynitrite, uric acid, and tested its effect on cisplatin-induced hydroxyl radical formation. Figure 4a and b shows that uric acid was able to inhibit the ESR signal induced by cisplatin, suggesting peroxynitrite decomposition as a potential source for hydroxyl radical formation in the test system.

Effects of cisplatin treatment on apoptosis-regulatory proteins

Cisplatin was previously shown to induce apoptosis through the mitochondrial death pathway [9, 33]. Since this pathway of apoptosis is known to be regulated by the balance of anti- and pro-apoptotic proteins in the Bcl-2 family [34, 35], we examined the expression level of two key Bcl-2 family proteins, namely Bcl-2 and Bax, in response to cisplatin treatment in HFDPC and HaCaT cells. Immunoblotting studies show that cisplatin induced down-regulation of the anti-apoptotic Bcl-2 protein and up-regulation of the pro-apoptotic Bax protein in a dose-dependent manner (Fig. 5a, b). We also measured the activation of caspase-3 by measuring the proteolytic cleavage of pro-caspase-3 protein and caspase-3 enzymatic activity in cisplatin-treated cells. The result shows that cisplatin was able to induce the processing of inactive pro-caspase-3 to active caspase-3, as indicated by the down-regulation of procaspase-3 (Fig. 5a, b) and the significant increase in caspase-3 activity (Fig. 5c, d). Since activation of caspase-3 is a critical execution step of caspase-dependent apoptosis [36, 37], the result of this study supports the induction of apoptosis by cisplatin through a caspase-dependent mechanism. The involvement of ROS in cisplatin-induced apoptosis was confirmed by the observation that an addition of NAC strongly inhibited the effects of cisplatin on apoptosis-regulatory proteins Bcl-2, Bax, and pro-caspase-3. Time dependence studies of the effect of cisplatin on Bcl-2 and Bax show that cisplatin induced a significant change in the protein levels at approximately 6 h after the treatment (Fig. 5c, d).

Cisplatin regulated Bcl-2 and Bax through hydroxyl radical

To determine the potential role of ROS in Bcl-2 and Bax regulation, the expression level of Bcl-2 and Bax after cisplatin treatment was determined in the presence or absence of NAC, CAT, MnTBAP, and sodium formate. In agreement with the apoptosis assay (Fig. 3a, b), Western blot analysis of Bcl-2 expression showed that the down-regulation of Bcl-2 by

cisplatin was inhibited by the addition of sodium formate or NAC, but not by CAT or MnTBAP (Fig. 6a, b). Sodium formate also inhibited the effect of cisplatin on Bax, whereas CAT had no significant effect and MnTBAP had variable effect. Together, these results suggest the role of hydroxyl radical as a key ROS involved in the alteration of Bcl-2 and Bax after cisplatin treatment.

Cisplatin induced Bcl-2 ubiquitination through hydroxyl radical

Bcl-2 has been shown to be regulated by ubiquitin-proteasomal degradation pathway under diverse apoptosis conditions [9, 26, 28]. To determine whether this pathway is involved in the down-regulation of Bcl-2 by cisplatin in the test cell systems, HFDPC and HaCaT cells were treated with lactacystin, a highly specific proteasome inhibitor, and its effects on cisplatin-induced Bcl-2 down-regulation was determined by western blotting. As lysosomal degradation is another possible pathway of protein degradation [38], cells were also treated with cisplatin in the presence or absence CMA, a known lysosome inhibitor. Figure 7a and b shows that lactacystin inhibited the down-regulation of Bcl-2 by cisplatin both in HFDPC and HaCaT cells, whereas CMA had no significant effect, suggesting proteasomal degradation as the primary mechanism of cisplatin-induced Bcl-2 down-regulation.

Ubiquitination is a major cellular process for selective removal of proteins via proteasomal degradation [39]. We tested whether cisplatin could induce Bcl-2 ubiquitination in the test cell systems and whether or not ROS play a role in this process. Cells were treated with cisplatin in the presence or absence of various ROS scavengers, and cell lysates were prepared and immunoprecipitated using anti-Bcl-2 antibody. The resulting immune complexes were then analyzed for ubiquitination using anti-ubiquitin antibody. The results show that cisplatin was able to induce Bcl-2 ubiquitination and that this effect was inhibited by the general antioxidant NAC or the hydroxyl scavenger sodium formate (Fig. 7c, d). Neither CAT nor MnTBAP was effective in inhibiting the ubiquitination, indicating that hydroxyl radical is the major oxidative species involved in the ubiquitination process.

Effect of ROS generation and Bcl-2 expression on cisplatin-induced apoptosis

Although a similar pattern of apoptosis was observed in HFDPC and HaCaT cells, the apoptotic response to cisplatin treatment in HFDPC cells was much lower than that in HaCaT cells (Fig. 8a). As ROS was earlier shown to be required for the induction of apoptosis by cisplatin, we tested the level of ROS generation in the two cell types after cisplatin treatment. Figure 8b shows that at the same treatment concentrations, HFDPC cells produced less ROS than HaCaT cells. However, at the IC_{25} concentration of cisplatin (about 100 μM in HFDPC cells and 25 μM in HaCaT cells), the cellular ROS level was about the same in the two cell types, suggesting a correlation between the ROS and apoptotic responses.

Bcl-2 was previously shown to be a key regulator of apoptosis induced by cisplatin in cancer cells [9]. We tested whether Bcl-2 also plays a role in the apoptosis regulation of non-cancer hair follicular cells. The cells were transfected with Bcl-2 or control plasmid, and their effect on cisplatin-induced apoptosis was examined. Because primary HFDPC cells were refractory to gene transfection, we used only HaCaT cells to study the role of Bcl-2 in the

apoptosis. Figure 8c and d shows that Bcl-2-transfected HaCaT cells expressed a higher level of Bcl-2 protein and exhibited less susceptibility to apoptosis induction by cisplatin than vector-transfected control cells. Analysis of ROS generation in these cells shows that Bcl-2-transfected cells produced less ROS than the control cells (Fig. 8e). Since hydroxyl radical was shown to be a key mediator of cisplatin-induced apoptosis, we further evaluated the potential antioxidant effect of Bcl-2 on hydroxyl radical generation in a well defined system using ferrous sulfate as a source of hydroxyl radical generation through Fenton reaction. Figure 8f shows that treatment of the cells with ferrous sulfate resulted in a substantial increase in ROS generation. However, this effect was less pronounced in Bcl-2-transfected cells as compared to vector-transfected cells. Together, these results support the role of Bcl-2 as a suppressor of cisplatin-induced apoptosis and as a negative regulator of hydroxyl radical generation.

Discussion

Chemotherapy-induced alopecia is a major clinical problem associated with most cancer chemotherapies. Despite improvements in CIA management and active research in recent years, effective treatment of CIA has yet to be developed and the mechanisms underlying the disease process remain poorly understood. It is generally accepted that CIA develops as a result of massive cell death of hair follicle cells after chemotherapy. Strategic intervention of this cell death, i.e., by localized treatment, may prevent or alleviate CIA without negatively affecting chemotherapy efficacy.

In the present study, we demonstrated that cisplatin induced toxicity of human HFDPC and keratinocytes through a mechanism that involves ROS-dependent apoptosis. The role of ROS in cisplatin toxicity was previously reported in renal proximal tubular cells and cochlear tissues, implicating in nephrotoxicity and ototoxicity [10–12, 14, 15]. Modulation of specific ROS pathways might protect cisplatin toxicity [40]. In dermal HFDPC and HaCaT cells, we found that ROS were generated in these cells in response to cisplatin treatment and that inhibition of ROS by antioxidant NAC or hydroxyl radical scavenger sodium formate effectively inhibited apoptosis induced by cisplatin, supporting the role of ROS, particularly hydroxyl radical, in the process. Although hydrogen peroxide was previously shown to be a key mediator of apoptosis induced by cisplatin in human lung cancer cells [9], we did not observe the same effect in the dermal cell systems. These results suggest that the specific ROS and apoptosis response to cisplatin treatment is cell type-specific and may be determined by the phenotypic characteristics of cells, i.e., their expression of antioxidant enzymes. It is worth noting that normal cells and cancer cells appear to have differential susceptibility to cisplatin-induced ROS generation and apoptosis, which may be exploited for selective killing of cancer cells while sparing normal cells. For example, selective inhibition of hydroxyl radicals without affecting peroxide formation, i.e., through the use of hydroxyl radical scavengers, could be envisioned to protect normal cells and promote the killing of cancer cells by cisplatin.

The mechanism of cisplatin-induced ROS generation is incompletely understood. In the present study, we found that hydroxyl radicals play a dominant role in dermal toxicity. Our results also suggested that peroxynitrite decomposition is a likely source of hydroxyl radical

formation. An elevated level of hydroxyl radicals could initiate a multitude of signaling cascades leading to apoptotic or necrotic cell death. Apoptosis was found to be the primary mode of cell death based on the ability of apoptosis (caspase) inhibitor, zVAD-fmk, to inhibit cisplatin-induced cell death, and the lack of necrosis in cisplatin-treated cells under the test conditions as determined by propidium iodide assay (data not shown).

Apoptosis induced by cisplatin has been shown to be mediated through the mitochondrial death pathway [9, 33]. Since Bcl-2 family proteins are known to be key regulators of this pathway and since Bcl-2 and Bax have been suggested to play a key role in hair follicle cell apoptosis [21, 22], we focused our efforts on these proteins and their regulation by ROS. We found that cisplatin induced down-regulation of Bcl-2 and up-regulation of Bax in concomitant with apoptosis, the effects that are dependent on ROS generation. The hydroxyl radical scavenger sodium formate effectively inhibited these effects, whereas other ROS scavengers including CAT and MnTBAP had no or minimal effects. These results indicate that hydroxyl radical is the major oxidative species responsible for Bcl-2 and Bax alterations and the induction of apoptosis by cisplatin in the test cell systems.

The anti-apoptotic function of Bcl-2 is closely associated with its expression level, which is controlled by various mechanisms depending on the apoptotic stimuli [25, 26]. Consistent with the previous reports [9, 41], our study shows that down-regulation of Bcl-2 by cisplatin is mediated mainly through the ubiquitin-proteasomal degradation pathway. Inhibition of ROS by formate but not by CAT or MnTBAP inhibited the ubiquitination of Bcl-2, indicating the dominant role of hydroxyl radical in the process.

We also observed the difference in apoptosis and ROS response to cisplatin treatment in HFDPC and HaCaT cells. The keratinocyte HaCaT cells were substantially more responsive than the dermal papilla HFDPC cells, suggesting that keratinocytes are the major target of cisplatin toxicity in hair follicle cells. Although apoptosis is controlled by several regulatory proteins, and down-regulation of Bcl-2 itself may be insufficient to induce apoptosis, we found that overexpression of Bcl-2 protects the cells from cisplatin-induced apoptosis. Furthermore, ROS induction by cisplatin was lower in Bcl-2-overexpressing cells as compared to vector-transfected cells, suggesting the potential antioxidant function of Bcl-2. The expression level of Bcl-2 was also found to be higher in HFDPC cells as compared to HaCaT cells (data not shown). Thus, Bcl-2 might contribute to some extent to the antioxidant defense mechanism of HFDPC cells. Since ROS generation is known to be a mechanism of action of cisplatin [8, 9], the results of this study reveal one possible mechanism of cisplatin resistance in Bcl-2-overexpressing cells.

In summary, our data provide evidence that hydroxyl radical is a key mediator of cisplatin-induced apoptosis in human HFDPC and HaCaT keratinocytes through a mechanism that involves Bcl-2 down-regulation and caspase activation, which has not been previously reported. Hydroxyl radical is the major oxidative species responsible for the down-regulation of Bcl-2 via ubiquitin-proteasomal degradation. Because ROS are induced by various chemotherapeutic agents such as doxorubicin and cyclophosphamide and are associated with their toxic side effects [42, 43], our findings on the mechanisms of apoptosis regulation by

ROS in the hair follicle cells could be important in the understanding of CIA by other drugs and in the development of novel therapeutic and preventive approaches for CIA.

Acknowledgments

This work was supported by the National Institutes of Health Grant R01-HL76340 (to Y.R.) and the Thailand Research Fund Grant RGJ-5.Q.CU/49/A.1 (to U.N.).

Abbreviations

CDDP	*cis*-diamminedichloroplatinum, cisplatin
HFDPC	Human hair follicle dermal papilla cells
ROS	Reactive oxygen species
hROS	Highly reactive oxygen species
MTT	3-(4,5-dimethylthiazol-2-yl)-2,5-diphenyltetrazolium bromide
zVAD-fmk	Benzyloxycarbonyl-Val-Ala-Asp-(OMe) fluoromethyl ketone
NAC	*N*-acetyl cysteine
GSH	Reduced glutathione
H_2DCF-DA	Dihydrodichlorofluorescein diacetate
HPF	Hydroxyphenyl fluorescein
CAT	Catalase
MnTBAP	Mn(III)tetrakis(4-benzoic acid) porphyrin chloride
NaFM	Sodium formate
Pro-C3	Pro-caspase-3
LAC	Lactacystin
CMA	Concanamycin A
Ub	Ubiquitin
SDS-PAGE	Sodium dodecyl sulfate-polyacrylamide gel electrophoresis

References

1. Trueb RM. Chemotherapy-induced alopecia. Semin Cutan Med Surg. 2009; 28:11–14. [PubMed: 19341937]
2. Carelle N, Piotto E, Bellanger A, Germanaud J, Thuillier A, Khayat D. Changing patient perceptions of the side effects of cancer chemotherapy. Cancer. 2002; 95:155–163. [PubMed: 12115329]
3. Wang J, Lu Z, Au JLS. Protection against chemotherapy-induced alopecia. Pharm Res. 2006; 23:2505–2514. [PubMed: 16972183]

4. Botchkarev VA. Molecular mechanisms of chemotherapy-induced hair loss. J Investig Dermatol Symp Proc. 2003; 8:72–75.
5. Jimenez JJ, Roberts SM, Mejia J, Lucia M, Mauro LM, Munson JW, et al. Prevention of chemotherapy-induced alopecia in rodent models. Cell Stress Chaperones. 2008; 13:31–38. [PubMed: 18347939]
6. Bodo E, Tobin DJ, Kamenisch Y, Biro T, Berneburg M, Funk W, et al. Dissecting the impact of chemotherapy on the human hair follicle: a pragmatic in vitro assay for studying the pathogenesis and potential management of hair follicle dystrophy. Am J Pathol. 2007; 171:1153–1167. [PubMed: 17823286]
7. Apisarnthanarax, N.; Duvic, M. Dermatologic complications of cancer chemotherapy. In: Bast, RC.; Kufe, DW.; Pollock, RE.; Weichselbaum, RR.; Holland, JF.; Frei, E., editors. Holland-Frei cancer medicine. 5th. Hamilton: BC Decker; 2000. p. 2271-2278.
8. Mijajima A, Nakashima J, Yoshioka K, Tachibana M, Tazaki H, Murai M. Role of reactive oxygen species in cis-dichlorodiammineplatinum-induced cytotoxicity in bladder cancer cells. Br J Cancer. 1997; 76:206–210. [PubMed: 9231920]
9. Wang L, Chanvorachote P, Toledo D, Stehlik C, Mercer RR, Castranova V, et al. Peroxide is a key mediator of Bcl-2 down-regulation and apoptosis induction by cisplatin in human lung cancer cells. Mol Pharmacol. 2008; 73:119–127. [PubMed: 17911532]
10. Clerici WJ, Hensley K, DiMartino DL, Butterfield DA. Direct detection of ototoxicant-induced reactive oxygen species generation in cochlear explants. Hear Res. 1996; 98:116–124. [PubMed: 8880186]
11. Rybak LP, Whitworth CA, Mukherjea D, Ramkumar V. Mechanisms of cisplatin-induced ototoxicity and prevention. Hear Res. 2007; 226:157–167. [PubMed: 17113254]
12. Pabla N, Dong Z. Cisplatin nephrotoxicity: mechanisms and renoprotective strategies. Kidney Int. 2008; 73:994–1007. [PubMed: 18272962]
13. Somani SM, Husain K, Whitworth C, Trammell GL, Malafa M, Rybak LP. Dose-dependent protection by lipoic acid against cisplatin-induced nephrotoxicity in rats: antioxidant defense systems. Pharmacol Toxicol. 2000; 86:234–241. [PubMed: 10862506]
14. Jiang M, Wei Q, Pabla N, Dong G, Wang CY, Yang T, et al. Effects of hydroxyl radical scavenging on cisplatin-induced p53 activation, tubular cell apoptosis, and nephrotoxicity. Biochem Pharmacol. 2007; 73:1499–1510. [PubMed: 17291459]
15. Santos NA, Bezerra CS, Martins NM, Curti C, Bianhi ML, Santos AC. Hydroxyl radical scavenger ameliorates cisplatin-induced nephrotoxicity by preventing oxidative stress, redox state unbalance, impairment of energetic metabolism and apoptosis in rat kidney mitochondria. Cancer Chemother Pharmacol. 2008; 61:145–155. [PubMed: 17396264]
16. Wu YJ, Muldoon LL, Neuwelt EA. The chemoprotective agent *N*-acetylcysteine blocks cisplatin-induced apoptosis through caspase signaling pathway. J Pharmacol Exp Ther. 2005; 312:424–431. [PubMed: 15496615]
17. Li P, Nijhawan D, Budihardjo I, Srinivasula S, Ahmad M, Alnemri E, et al. Cytochrome c and dATP-dependent formation of Apaf-1/caspase-9 complex initiates an apoptotic protease cascade. Cell. 1997; 91:479–489. [PubMed: 9390557]
18. Gupta S. Molecular signaling in death receptor and mitochondrial pathways of apoptosis. Int J Oncol. 2003; 22:15–20. [PubMed: 12469180]
19. Korsmeyer SJ, Yin XM, Oltvai ZN, Veis-Novack DJ, Linette GP. Reactive oxygen species and the regulation of cell death by the Bcl-2 gene family. Biochim Biophys Acta. 1995; 1271:63–66. [PubMed: 7599227]
20. Martin SS, Vuori K. Regulation of Bcl-2 proteins during anoikis and amorphosis. Biochim Biophys Acta. 2004; 1692:145–157. [PubMed: 15246684]
21. Muller-Rover S, Rossiter H, Lindner G, Peters EMJ, Kupper TS, Paus R. Hair follicle apoptosis and Bcl-2. J Investig Dermatol Symp Proc. 1999; 4:272–277.
22. Botchkareva NV, Ahluwalia G, Shander D. Apoptosis in the hair follicle. J Invest Dermatol. 2006; 126:258–264. [PubMed: 16418734]

23. Yang X, Zheng F, Xing H, Gao Q, Wei W, Lu Y, et al. Resistance to chemotherapy-induced apoptosis via decreased caspase-3 activity and overexpression of antiapoptotic proteins in ovarian cancer. Cancer Res Clin Oncol. 2004; 130:423–428.
24. Kausch I, Jiang H, Thode B, Doehn C, Kruger S, Joeham D. Inhibition of Bcl-2 enhances the efficacy of chemotherapy in renal cell carcinoma. Eur Urol. 2005; 47:703–709. [PubMed: 15826766]
25. Dimmeler S, Breitschopf K, Haendeler J, Zeiher AM. Dephosphorylationtargets Bcl-2 for ubiquitin-dependent degradation: a link between the apoptosome and the proteasome pathway. J Exp Med. 1999; 189:1815–1822. [PubMed: 10359585]
26. Chanvorachote P, Nimmannit U, Stehlik C, Wang L, Jiang BH, Ongpipatanakul B, et al. Nitric oxide regulates cell sensitivity to cisplatin-induced apoptosis through *S*-nitrosylation and inhibition of Bcl-2 ubiquitination. Cancer Res. 2006; 66:6353–6360. [PubMed: 16778213]
27. Haendeler J, Messmer UK, Brune B, Neugebauer E, Dimmeler S. Endotoxic shock leads to apoptosis in vivo and reduces Bcl-2. Shock. 1996; 6:405–409. [PubMed: 8961390]
28. Azad N, Iyer AKV, Manosroi A, Wang L, Rojanasakul Y. Superoxide-mediated proteasomal degradation of Bcl-2 determines cell susceptibility to Cr(VI)-induced apoptosis. Carcinogenesis. 2008; 29:1538–1545. [PubMed: 18544562]
29. Inui S, Itami S, Pan HJ, Chang C. Lack of androgen receptor transcriptional activity in human keratinocytes. J Dermatol Sci. 2000; 23:87–92. [PubMed: 10808125]
30. Setsukinai K, Urano Y, Kakinuma K, Majima HJ, Nagano T. Development of novel fluorescence probes than can reliably detect reactive oxygen species and distinguish specific species. J Biol Chem. 2003; 278:3170–3175. [PubMed: 12419811]
31. Beckman JC, Beckman TW, Chen J, Marshall PA, Freeman BA. Apparent hydroxyl radical production by peroxynitrite: implications for endothelial injury from nitric oxide and superoxide. Proc Natl Acad Sci USA. 1997; 87:1620–1624.
32. Zhang H, Joseph J, Feix J, Hogg N, Kalyanaraman B. Nitration and oxidation of a hydrophobic tyrosine probe by peroxynitrite in membranes: comparison with nitration and oxidation of tyrosine by peroxynitrite in aqueous solution. Biochemistry. 2001; 40:7675–7686. [PubMed: 11412121]
33. Park MS, Leon MD, Devarajan P. Cisplatin induces apoptosis in LLC-PK1 cells via activation of mitochondrial pathways. J Am Soc Nephrol. 2002; 13:858–865. [PubMed: 11912244]
34. Mignotte B, Vayssiere JL. Mitochondria and apoptosis. Eur J Biochem. 1998; 252:1–15. [PubMed: 9523706]
35. Tsujimoto Y. Role of Bcl-2 family proteins in apoptosis: apoptosomes or mitochondria. Genes Cell. 1998; 3:697–707.
36. Porter AG, Janicke RU. Emerging roles of caspase-3 in apoptosis. Cell Death Differ. 1999; 6:99–104. [PubMed: 10200555]
37. Elmore S. Apoptosis: a review of programmed cell death. Toxicol Pathol. 2007; 35:495–516. [PubMed: 17562483]
38. Ciechanover A. Proteolysis: from the lysosome to ubiquitin and the proteasome. Nat Rev Mol Cell Biol. 2005; 6:79–86. [PubMed: 15688069]
39. Lecker SW, Goldberg AL, Mitch WE. Protein degradation by the ubiquitin-proteasomal pathway in normal and disease states. J Am Soc Nephrol. 2006; 17:1807–1819. [PubMed: 16738015]
40. McFadden SL, Ding D, Salvemini D, Salvi RJ. M40403, a superoxide dismutase mimetic, protects cochlear hair cells from gentamicin, but not cisplatin toxicity. Toxicol Appl Pharmacol. 2003; 186:46–54. [PubMed: 12583992]
41. Li D, Ueta E, Kimura T, Yamamoto T, Osaki T. Reactive oxygen species (ROS) control the expression of Bcl-2 family proteins by regulating their phosphorylation and ubiquitination. Cancer Sci. 2004; 95:644–650. [PubMed: 15298726]
42. Wang S, Kanorev EA, Kotamraju S, Joseph J, Kalivendi S, Kalyanaraman B. Doxorubicin induces apoptosis in normal and tumor cells via distinctly different mechanisms. J Biol Chem. 2004; 279:25535–25543. [PubMed: 15054096]
43. Korkmaz A, Topol T, Oter S. Pathophysiological aspects of cyclophosphamide and ifosphamide induced hemorrhagic cystitis; implication of reactive oxygen species and nitrogen species as well as PARP activation. Cell Biol Toxicol. 2007; 23:303–312. [PubMed: 17225077]

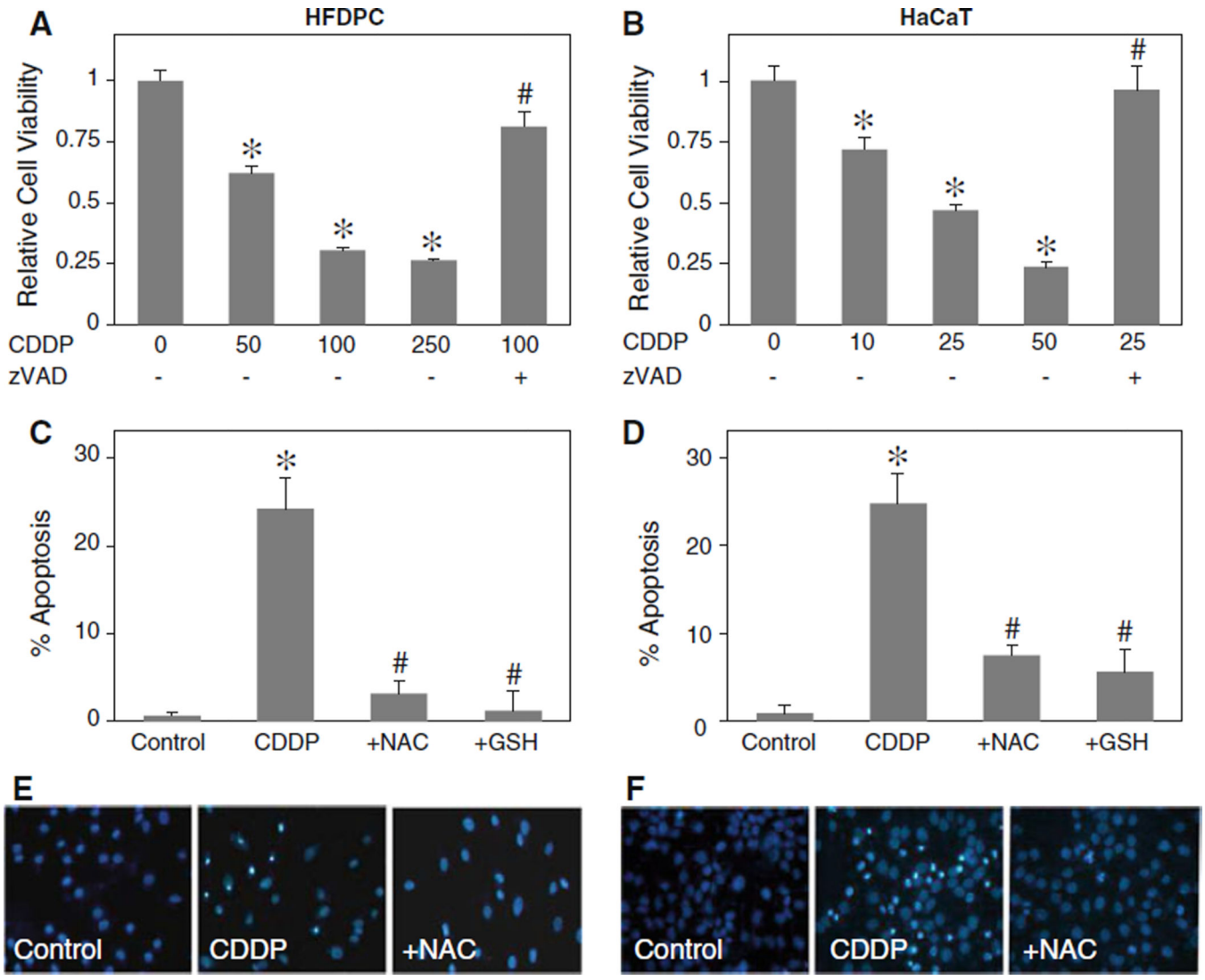

Fig. 1.

Cisplatin induces toxicity of human HFDPC and HaCaT keratinocytes by apoptosis. **a, b** Subconfluent monolayers (80%) of HFDPC and HaCaT cells were treated with various concentrations of cisplatin (CDDP; 0–250 and 0–50 μM in HFDPC and HaCaT cells, respectively) in the presence or absence of pan-caspase inhibitor (z-VAD-fmk; 10 μM) for 24 h. Cell toxicity was then determined by MTT assay. **c, d** HFDPC and HaCaT cells were treated with cisplatin (100 and 25 μM in HFDPC and HaCaT cells, respectively) for 24 h in the presence or absence of NAC (2.5 mM) or GSH (2.5 mM) and analyzed for apoptosis by Hoechst 33342 assay. **e, f** Fluorescence micrographs of the treated cells stained with Hoechst dye. Apoptotic cells exhibited condensed and/or fragmented nuclei with bright nuclear fluorescence (original magnification, ×400). *Plots* are mean ± SD ($n = 4$). *$P < 0.05$ versus non-treated control. #$P < 0.05$ versus cisplatin-treated control

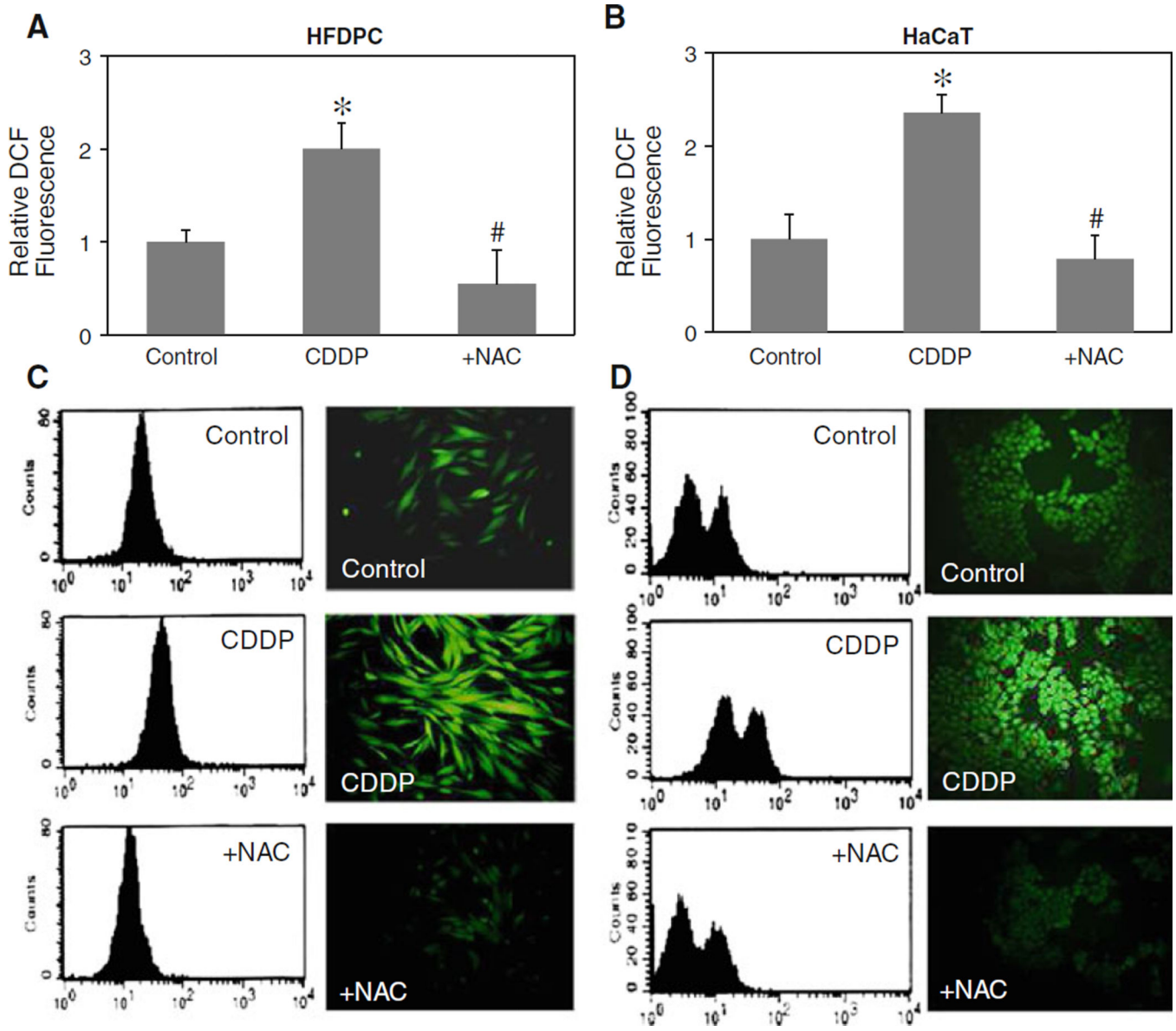

Fig. 2.

Effect of cisplatin on cellular ROS generation. **a, b** HFDPC and HaCaT cells were treated with cisplatin (100 and 25 μM in HFDPC and HaCaT cells, respectively) in the presence or absence of NAC (2.5 mM) for 2 h, after which they were analyzed for ROS generation by flow cytometry using H_2DCF-DA as a fluorescent probe. **c, d** Representative flow cytometric histograms (*left*) and fluorescence micrographs (*right*) of DCF measurements in the treated cells (original magnification, ×400). *Plots* are mean ± SD ($n = 3$). *$P < 0.05$ versus non-treated control. #$P < 0.05$ versus cisplatin-treated control

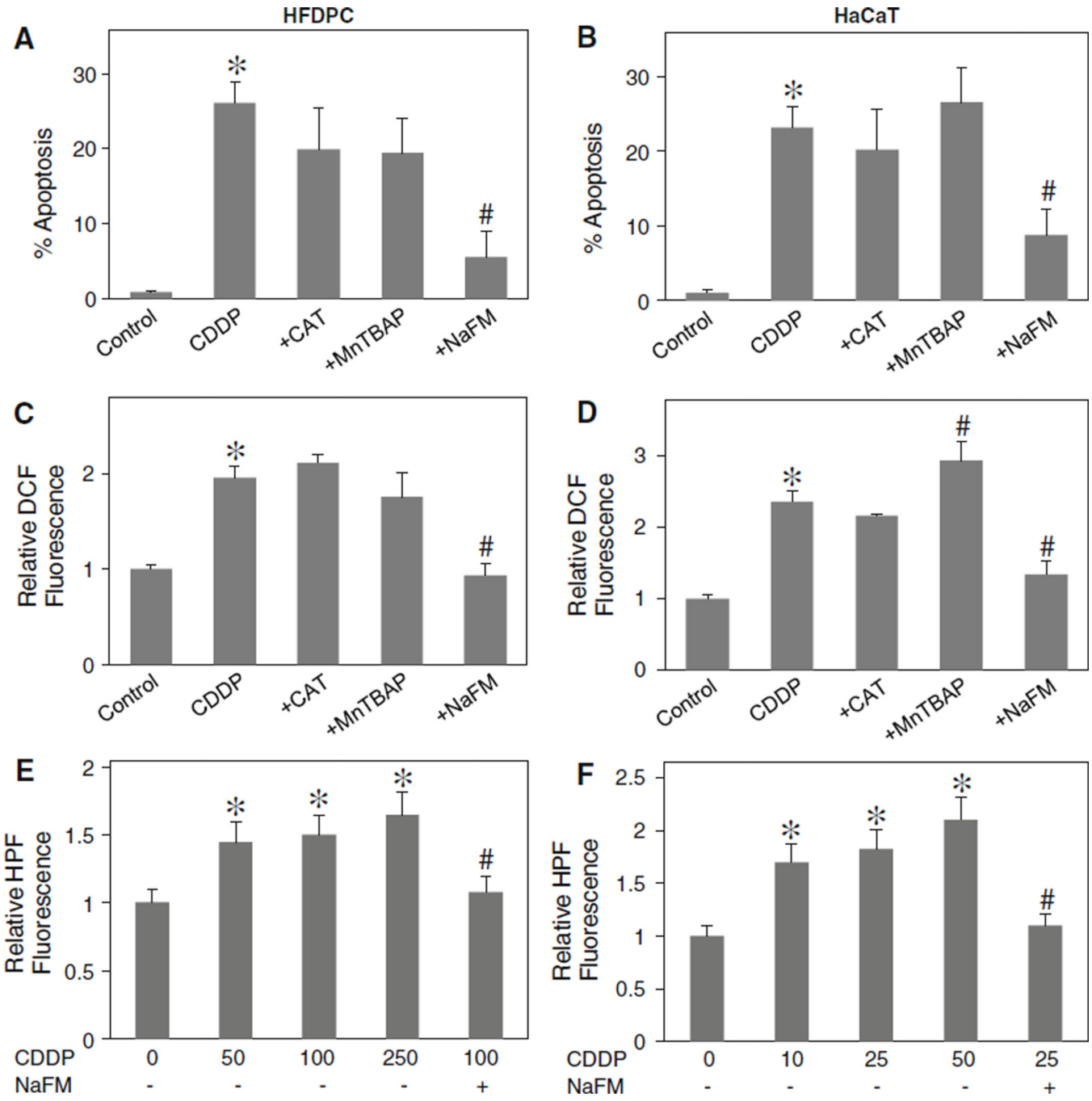

Fig. 3.

Effects of antioxidants on cisplatin-induced apoptosis and ROS generation. **a, b** HFDPC and HaCaT cells were pretreated for 30 min with CAT (7,500 U/ml), MnTBAP (50 μM), or sodium formate (NaFM, 2.5 mM) followed by cisplatin treatment (100 and 25 μM in HFDPC and HaCaT cells, respectively) for 24 h and analyzed for apoptosis by Hoechst 33342 assay. Increasing the dose of CAT or MnTBAP had no significant effect on the apoptotic signals (not shown). **c, d** HFDPC and HaCaT cells were similarly treated with the antioxidants and cisplatin as described above and analyzed for ROS generation at the

maximum response time of 2 h by flow cytometry using H_2DCF-DA as a fluorescent probe. Increasing the dose of antioxidants had no further effect on the ROS generation (not shown). **e, f** HFDPC and HaCaT cells were treated with various concentration of cisplatin (0–250 and 0–50 μM in HFDPC and HaCaT cells, respectively) in the presence or absence of sodium formate (2.5 mM) for 30 min and cellular hROS generation was determined by fluorescence plate reader using HPF as a fluorescent probe as described in "Material and methods" section. *Plots* are mean ± SD ($n = 4$). $^{*}P < 0.05$ versus non-treated control. $^{\#}P < 0.05$ versus cisplatin-treated control

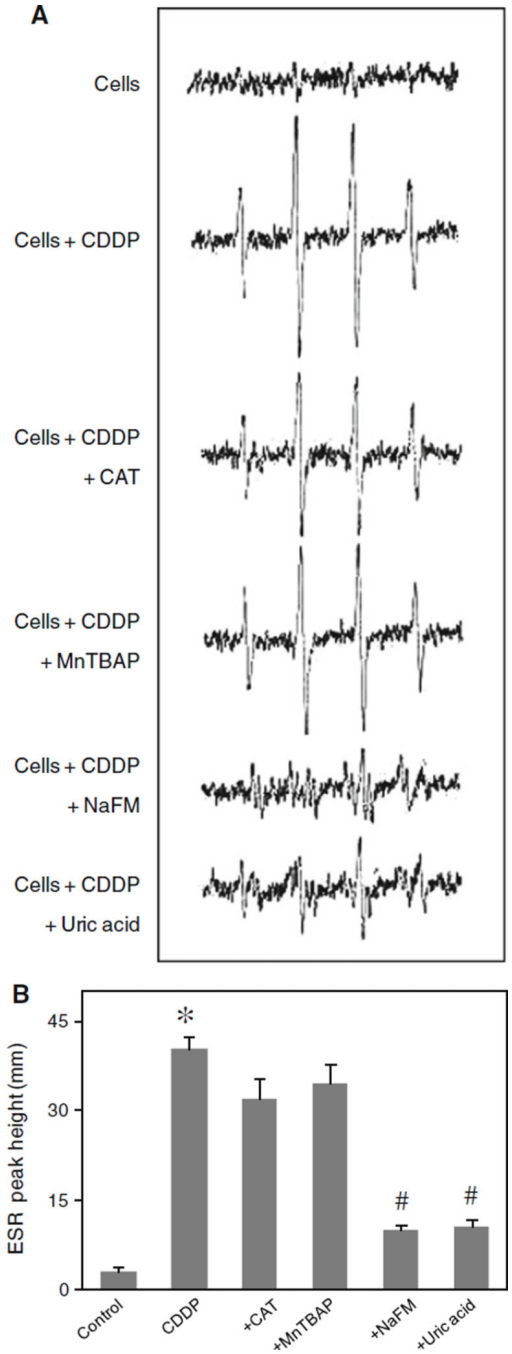

Fig. 4.

Hydroxyl radical induction by cisplatin treatment. **a** HaCaT cells (1×10^6 cells/ml) were incubated in PBS containing the spin trapper DMPO (10 mM) with or without cisplatin (25 μM), CAT (7,500 U/ml), MnTBAP (50 μM), sodium formate (NaFM, 2.5 mM), and uric acid (100 μM). ESR spectra were then recorded 30 min after the addition of the test agents. The spectrometer settings were as follows: receiver gain at 1.5×10^5, time constants at 0.3 s, modulation amplitude at 1.0 G, scan time at 4 min, and magnetic field at 3,470 ± 100 G. **b**

Analysis of ESR measurements. *Plots* are mean ± SD ($n = 3$). *$P < 0.05$ versus non-treated control (cells). #$P < 0.05$ versus cisplatin-treated control

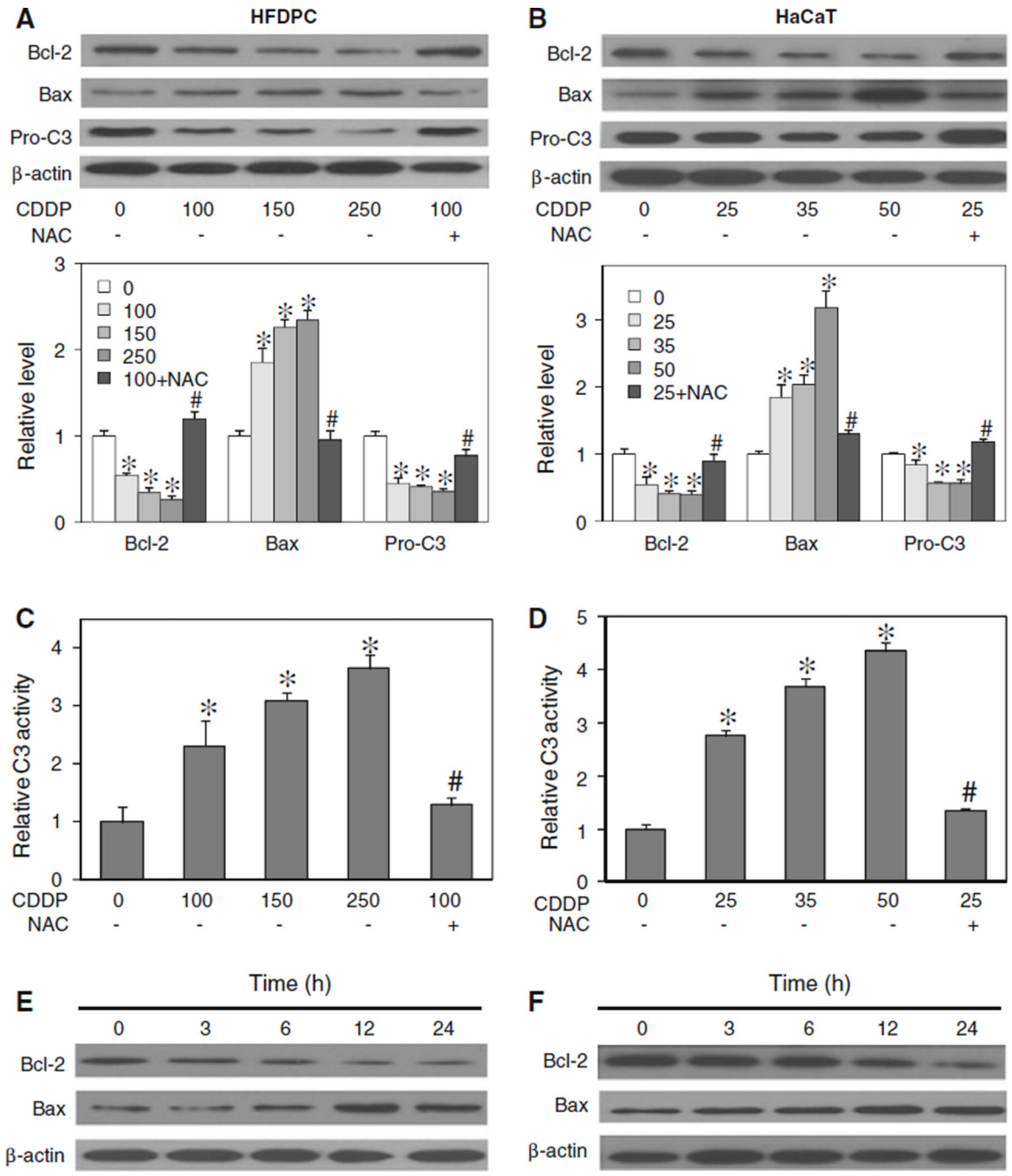

Fig. 5.

Effect of cisplatin treatment on apoptosis-regulatory proteins. **a, b** HFDPC and HaCaT cells were treated with cisplatin (0–250 and 0–50 μM in HFDPC and HaCaT cells, respectively) in the presence or absence of NAC (2.5 mM) for 24 h. Cell lysates were prepared and analyzed for Bcl-2, Bax, and pro-caspase 3 (Pro-C3) expression by western blotting. Blots were reprobed with β-actin antibody to confirm equal loading of samples. Immunoblot signals were quantified by densitometry, and mean data from three independent experiments (one of which is shown here) was normalized to the result obtained in cells without

treatment (control). **c, d** HFDPC and HaCaT cells were similarly treated with cisplatin in the presence or absence of NAC for 15 h, and analyzed for caspase-3 activity using the fluorometric substrate FAM-DEVD-fmk. **e, f** HFDPC and HaCaT cells were treated with cisplatin (100 and 25 μM in HFDPC and HaCaT cells, respectively) for various times (0–24 h), and Bcl-2 and Bax expression was determined. *Plots* are mean ± SD ($n = 3$). $^{*}P < 0.05$ versus non-treated control. $^{\#}P < 0.05$ versus cisplatin-treated control

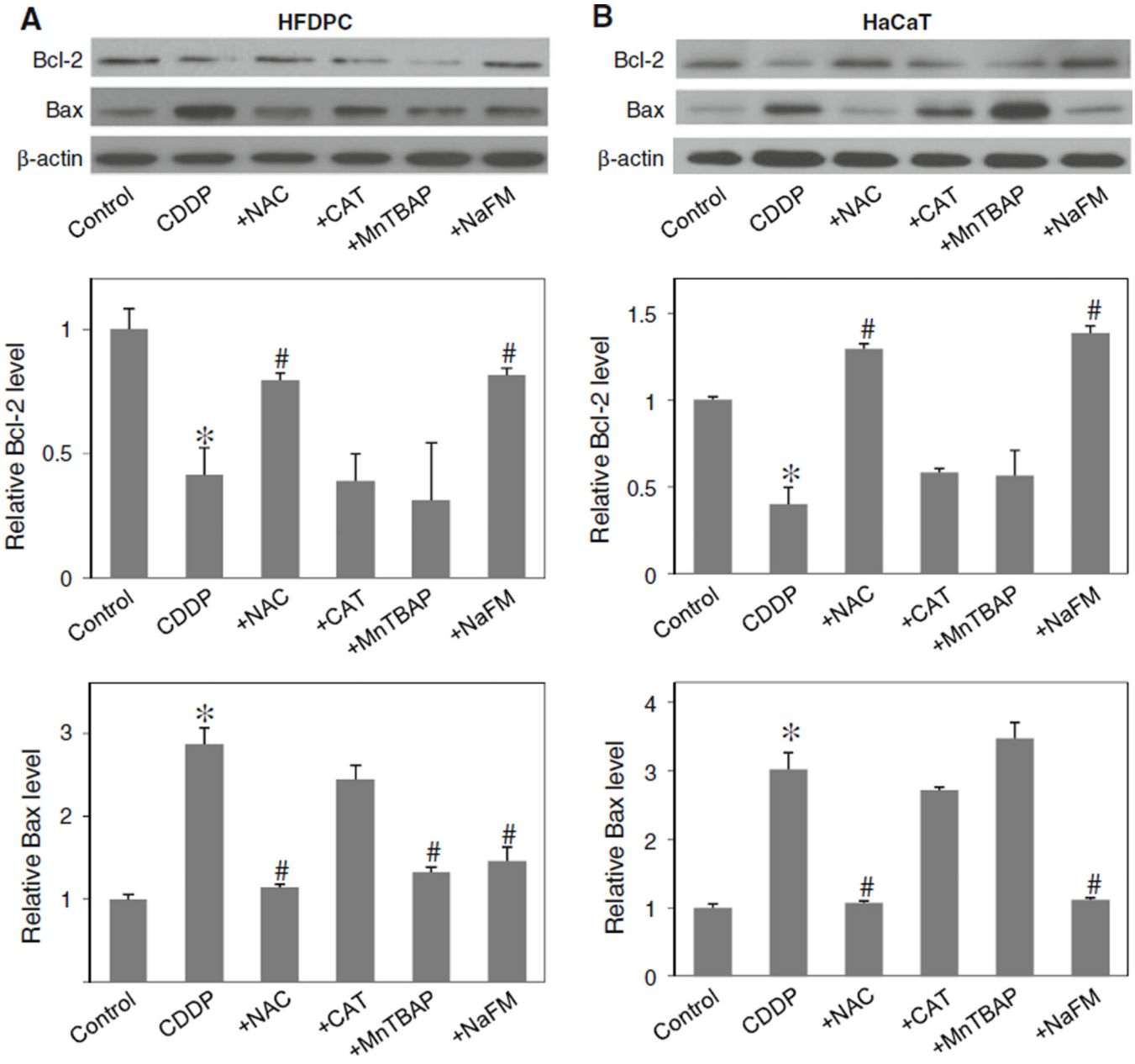

Fig. 6.

Effects of cisplatin and antioxidants on Bcl-2 and Bax expression. **a, b** HFDPC and HaCaT cells were treated with cisplatin (100 and 25 μM in HFDPC and HaCaT cells, respectively) in the presence or absence of NAC (2.5 mM), CAT (7,500 U/ml), MnTBAP (50 μM), or sodium formate (NaFM, 2.5 mM). Cell lysates were prepared and analyzed for Bcl-2 and Bax expression by western blotting using Bcl-2 and Bax antibodies. β-actin was used as a loading control. *Plots* are mean ± SD ($n = 3$). *$P < 0.05$ versus non-treated control. $^{\#}P < 0.05$ versus cisplatin-treated control

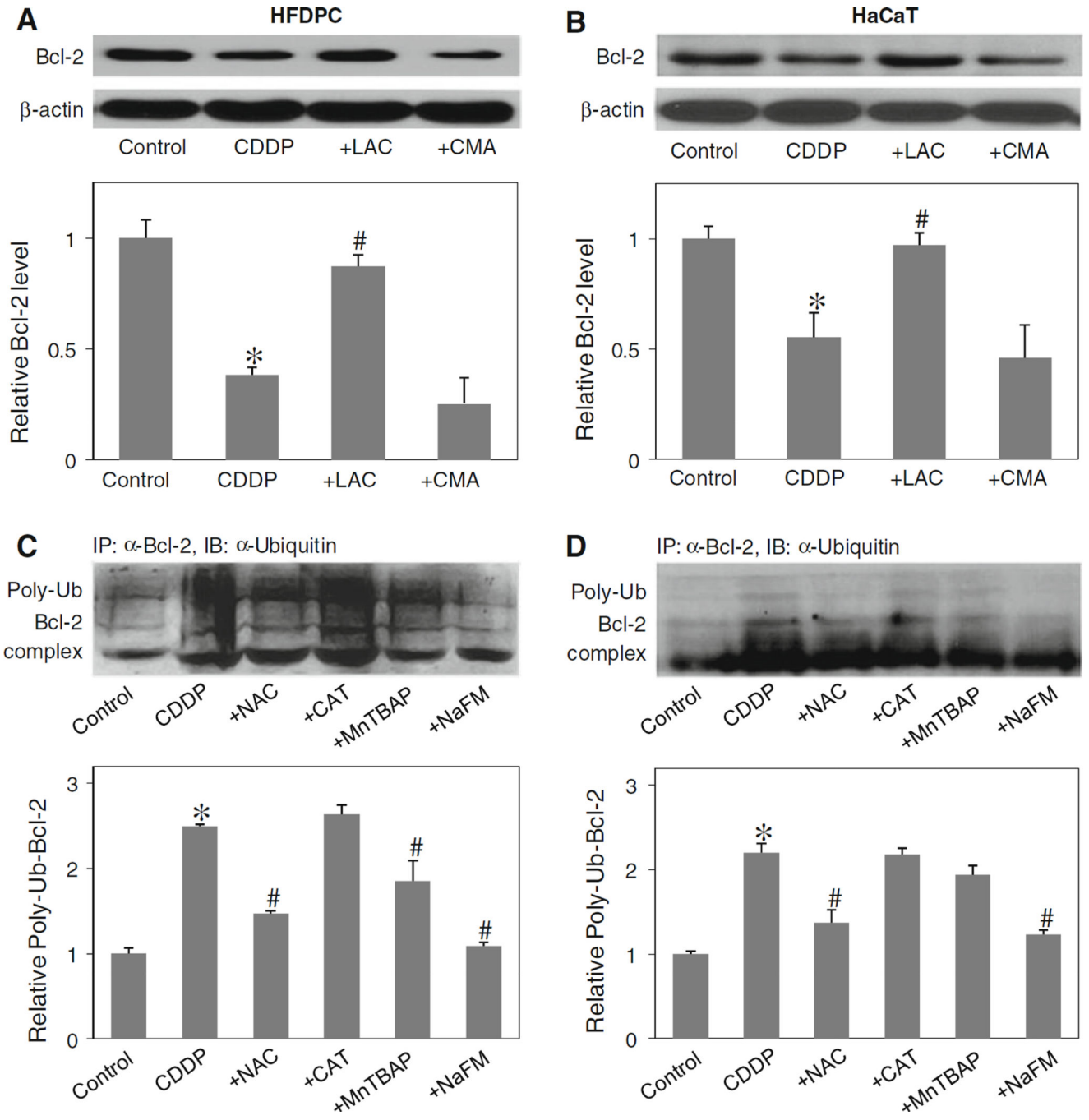

Fig. 7.

Effect of cisplatin and antioxidants on Bcl-2 ubiquitination. **a, b** HFDPC and HaCaT cells were pretreated with proteasome inhibitor lactacystin (LAC, 10 μM) or with lysosome inhibitor CMA (1 μM) for 1 h, and then treated with cisplatin (100 and 25 μM in HFDPC and HaCaT cells, respectively) for 24 h. Bcl-2 expression was determined by Western blots using anti-Bcl-2 antibody. **c, d** HFDPC and HaCaT cells were pretreated with LAC (10 μM) for 1 h (to prevent proteasomal degradation of Bcl-2) and then treated with cisplatin in the presence or absence of NAC (2.5 mM), CAT (7,500 U/ml), MnTBAP (50 μM), or sodium

formate (NaFM, 2.5 mM) for 2 h. Cell lysates were immunoprecipitated with anti-Bcl-2 antibody and the immune complexes were analyzed for ubiquitin by western blotting. Analysis of ubiquitin was performed at 2 h post-treatment where ubiquitination was found to be maximal. *Plots* are mean ± SD ($n = 3$). $^{*}P < 0.05$ versus non-treated control. $^{\#}P < 0.05$ versus cisplatin-treated control

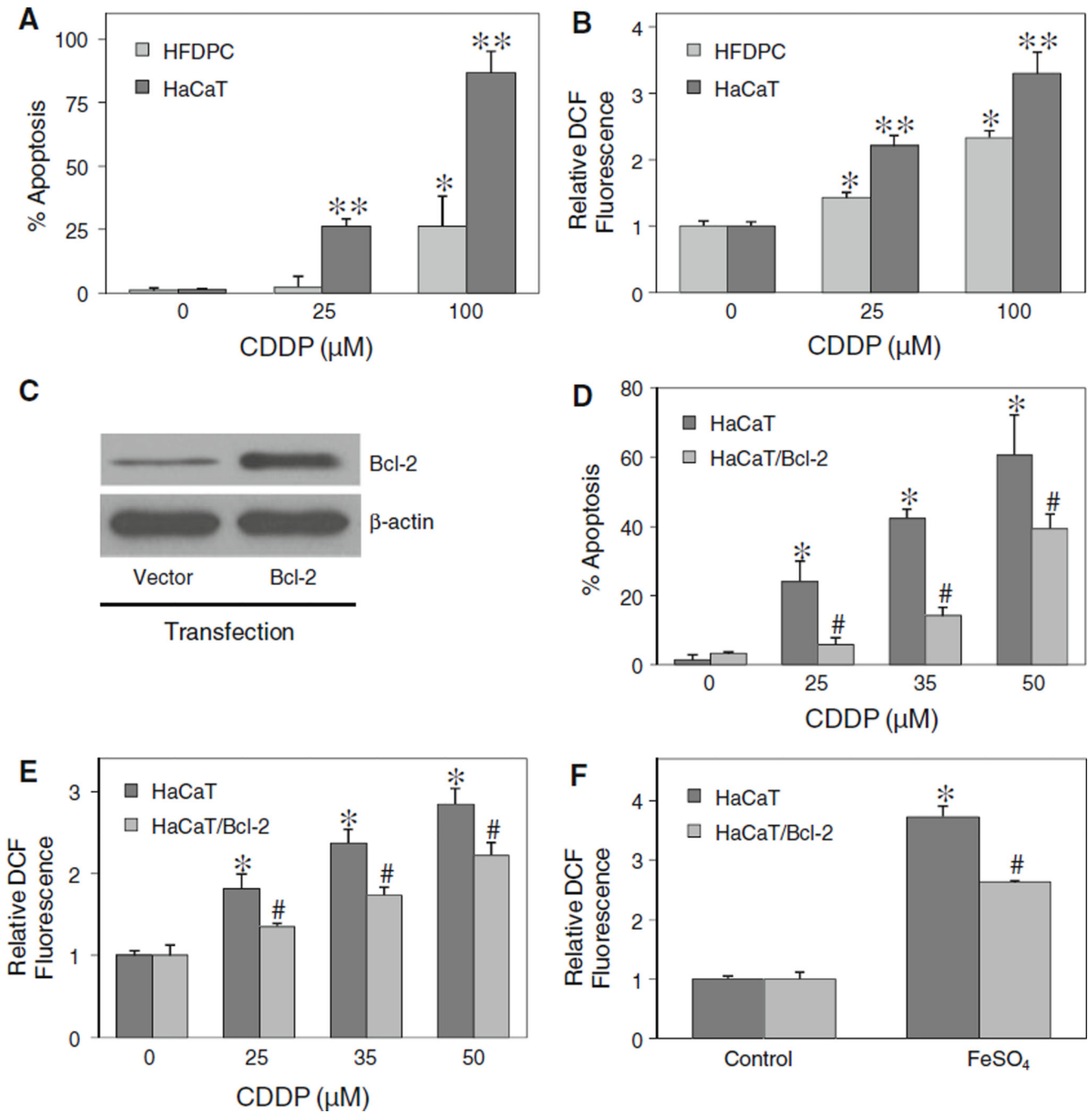

Fig. 8.

Effect of ROS generation and Bcl-2 expression on cisplatin-induced apoptosis. **a** HFDPC and HaCaT cells were treated with various concentrations of cisplatin (0–100 μM) for 24 h, and analyzed for apoptosis by Hoechst 33342 assay. **b** HFDPC and HaCaT cells were similarly treated with cisplatin and analyzed for ROS generation by flow cytometry at 2 h post-treatment. **c** HaCaT cells were transiently transfected with Bcl-2 or control pcDNA3 plasmid as described under “Material and methods” section. Transfected cells were analyzed for Bcl-2 expression by western blotting. **d** Transfected cells were treated with cisplatin (0–

50 μM) for 24 h and analyzed for apoptosis by Hoechst 33342 assay. **e** Transfected cells were similarly treated with cisplatin and analyzed for ROS generation by flow cytometry at 2 h after the treatment. **f** Transfected cells were treated with ferrous sulfate ($FeSO_4$, 100 μM) and ROS generation was similarly determined after 2 h. *Plots* are mean ± SD ($n = 3$). *$P <$ 0.05 versus non-treated control. $P < 0.05$ versus cisplatin-treated HFDPC cells. #$P < 0.05$ versus cisplatin-treated vector-transfected HaCaT cells